Br J Dermatol 2024; **00**:1–9
https://doi.org/10.1093/bjd/ljae196
Advance access publication date: 13 May 2024

BJD
British Journal of Dermatology
Surgical Dermatology

Diagnostic accuracy of autofluorescence-Raman microspectroscopy for surgical margin assessment during Mohs micrographic surgery of basal cell carcinoma

Radu A Boitor,[1] Sandeep Varma,[2] Ashish Sharma,[2] Sunita Odedra,[2] Somaia Elsheikh,[3] Karim Eldib,[3] Anand Patel,[2] Alexey Koloydenko,[4] Sonia Gran,[5] Koen De Winne,[6] Senada Koljenovic,[6] Hywel C Williams[5] and Ioan Notingher[1]

[1]School of Physics and Astronomy, University of Nottingham, Nottingham, UK
[2]Nottingham NHS Treatment Centre, Nottingham University Hospitals, Nottingham, UK
[3]Department of Pathology, Nottingham University Hospitals NHS Trust, Nottingham, UK
[4]Mathematics Department, Royal Holloway, University of London, UK
[5]Centre of Evidence-Based Dermatology, Lifespan and Population Health, School of Medicine, University of Nottingham, Nottingham, UK
[6]Department of Pathology, University of Antwerp and Antwerp University Hospital, Edegem, Belgium

Correspondence: Ioan Notingher. Email: ioan.notingher@nottingham.ac.uk

Abstract

Background Autofluorescence (AF)–Raman microspectroscopy is a technology that can detect residual basal cell carcinoma (BCC) on the resection margin of fresh, surgically excised tissue specimens. The technology does not require tissue fixation, staining, labelling or sectioning, and provides quantitative diagnosis maps of the surgical margins in 30 min.

Objectives To determine the accuracy of the AF–Raman instrument in detecting incomplete BCC excisions during Mohs micrographic surgery (MMS), using histology as the reference standard.

Methods Skin layers from 130 patients undergoing MMS at the Nottingham University Hospitals NHS Trust (September 2022–July 2023) were investigated with the AF–Raman instrument. The layers were measured when fresh, immediately after excision. The AF–Raman results and the intraoperative assessment by Mohs surgeons were compared with a postoperative consensus-derived reference produced by three dermatopathologists. The sensitivity, specificity, and positive and negative predictive values were calculated. The study was registered with ClinicalTrials.gov (NCT03482622).

Results AF–Raman analysis was successfully completed for 125 of 130 layers and, on average, covered 91% of the specimen surface area, with the lowest surface area covered being 87% for the eyelid and the highest being 94% for forehead specimens. The AF–Raman instrument identified positive margins in 24 of 36 BCC-positive cases [67% sensitivity, 95% confidence interval (CI) 49–82] and negative margins in 65 of 89 BCC-negative cases (73% specificity, 95% CI 63–82). Only one of 12 false-negative cases was caused by misclassification by the AF–Raman algorithm. The other 11 false-negatives cases were a result of no valid Raman signal being recorded at the location of the residual BCC due to either occlusion by blood or poor contact between tissue and the cassette window. The intraoperative diagnosis by Mohs surgeons identified positive margins in 31 of 36 BCC-positive cases (86% sensitivity, 95% CI 70–95) and negative margins in 79 of 89 BCC-negative cases (89% specificity, 95% CI 81–95).

Conclusions The AF–Raman instrument has the potential to provide intraoperative microscopic assessment of surgical margins in BCC surgery. Further improvements are required for tissue processing, to ensure complete coverage of the surgical specimens.

Lay summary

Basal cell carcinoma (BCC) is one of the most common human cancers, occurring mostly on the face and neck. Most BCCs are treated by cutting them out under local anaesthetic. This is routinely done in a hospital by a dermatologist or plastic surgeon. Surgery aims to remove all the cancer leaving the smallest scar possible, but it is often difficult to know how much normal skin to remove. Results from the laboratory often take 1 to 2 weeks to show if the cancer is clear.

A technique called 'Mohs' (micrographic surgery) is recommended for these 'high-risk' BCCs. Mohs surgery removes thin layers of skin and investigates them under a microscope while the patient is still in the hospital. This is repeated until all the layers are clear of cancer. Because of the patchy availability of Mohs surgery, many patients with high-risk BCCs are treated by traditional methods that may not be as good as Mohs.

We have developed an instrument that scans layers of skin and can quickly detect BCC. The instrument allows surgeons to check each removed skin layer for cancer cells to decide if more layers need to be removed. In this study, the instrument was tested on skin

Accepted: 4 May 2024

tissue layers from 130 patients who had Mohs surgery at the Nottingham Treatment Centre. The results showed that the instrument can measure skin layers in approximately 30 minutes and identify BCC with a similar accuracy to a Mohs surgeon, but only when the skin layers are prepared properly.

With future improvements, the technology might be used to guide Mohs surgery or help surgeons in centres that do not have access to Mohs surgery.

What is already known about this topic?

- Autofluorescence (AF)–Raman microspectroscopy has been shown to identify residual basal cell carcinoma (BCC) on frozen and fresh skin specimens immediately after excision by Mohs surgery.
- Previously published studies have shown the proportion of the tissue surface area investigated by AF–Raman can be higher than 90% and that it can detect the main subtypes of BCC.

What does this study add*?*

- This study presents the first diagnostic test of the accuracy of AF–Raman in detecting residual BCC on a set of full-face Mohs tissue layers resected from 125 patients.
- Once optimized, AF–Raman could be used for intraoperative margin control in BCC excision.

Basal cell carcinoma (BCC) accounts for approximately 90% of all keratinocyte cancers, with an increasing annual incidence.[1–4] The most widely available treatment for BCC is wide local excision (WLE), followed by histological examination of the surgical margins. A recent systematic review found that excision with 5 mm, 4 mm, 3 mm and 2 mm margins led to complete excision rates of 94.7%, 92.2%, 90.3% and 88.2%, respectively.[5] For high-risk BCCs on the head and neck, a 4–5-mm surgical margin may be difficult to achieve because of cosmetic or anatomical constraints.

Multiple studies have shown that 99% cure rates can be achieved by using a surgical margin of 1 or 2 mm of normal skin through Mohs micrographic surgery (MMS).[6] MMS has lower recurrence rates than WLE (4.4% vs. 12.2% after 10 years) and provides better conservation of uninvolved tissue.[3,7,8] However, the availability of MMS is patchy, owing to the limited number of trained Mohs surgeons and technician capacity to both process and assess histologically stained tissue sections intraoperatively.[5]

The increasing number of patients with high-risk BCCs requiring MMS puts a strain on the healthcare providers, with waiting times exceeding 120 days in England suggesting a need for additional margin-assessment techniques.[9]

Raman microspectroscopy has previously been shown to discriminate between BCC and healthy skin with 90–100% sensitivity and 85–92% specificity.[10–12] This discrimination is based on endogenous molecular differences between BCC and normal tissue, mainly associated with enlarged nuclei and protein signals, including collagen changes.[10–12] The main drawback of Raman microspectroscopy in biomedical applications is its weak signal, which leads to long measurement times. By combining Raman microspectroscopy with autofluorescence (AF) imaging, AF can be used to determine the main spatial features of the tissue sample. This information is then used to select and prioritize the sampling points for Raman microspectroscopy.

In a selective sampling approach, the measurement time is substantially expedited, allowing measurement of centimetre-sized tissue specimens in 30 min.[12–15] Based on this technology, we have previously reported the development and optimization of the table-top AF–Raman prototype instrument for clinical use.[13,14]

We recently conducted a pilot study on 50 fresh Mohs tissue layers from 50 patients. Layers were investigated immediately after excision and were measured either as split (27 layers) or as full-face (23 layers).[15] The instrument was able to scan skin tissue specimens from all anatomical locations relevant to MMS and detect the main BCC subtypes.

In this prospective study, we carried out the first diagnostic test of accuracy with the AF–Raman instrument, using postoperative histology as the reference standard.

Patients and methods

Patient recruitment and specimen collection

For this prospective cross-sectional study, 174 patients undergoing MMS at the Nottingham University Hospitals (NUH) National Health Service (NHS) Treatment Centre were recruited between September 2022 and July 2023 (56% female, 44% male). The study included the first-stage Mohs tissue layers from patients treated by four surgeons (S.V., A.S., S.O. and A.P.). Patients were included randomly, irrespective of age, sex or anatomical location of the lesion, provided their specimens met the study inclusion criteria outlined in the study protocol (Appendix S1; see Supplementary Information).[16] Forty-four specimens from the 174 recruited patients did not meet the inclusion criteria: patients were either the first to be operated on the day; their layers were larger than the AF–Raman cassette (2×2 cm^2); or the layers were too fragile to be blotted a minimum of 10 times. Therefore, the study dataset comprised 130 tissue

specimens from 130 patients. The study was registered with ClinicalTrials.gov (NCT03482622).

Tissue processing and autofluorescence–Raman measurements

The AF–Raman instrument (developed in collaboration with RiverD International, Rotterdam, the Netherlands)[13–15] was utilised in the Dermatology Department at the NUH NHS Treatment Centre. The specimens were excised, preprocessed, loaded in tissue cassettes and measured as full-face specimens, as previously reported.[15] Preprocessing required tissue specimens to be blotted to remove superficial blood. On average, tissue preprocessing took 3 min (maximum 6 min). The AF–Raman measurement and data analysis were fully automated and required no user intervention or data interpretation. The AF–Raman instrument produced diagnosis maps within 30 minutes, on average (further described in Appendix S1), with detected tumour represented as red regions on the map and normal tissue depicted in grey. Regions not investigated by the AF–Raman instrument because of the presence of superficial blood or inadequate contact between the specimen and the cassette window were presented in yellow and blue, respectively. After AF–Raman analysis, specimens were removed from the cassette and followed standard processing for frozen section histology (further detailed in Appendix S1).

Consensus-based reference standard

The AF–Raman microspectroscopy results were compared with postoperative histology, which represented the standard of reference. To account for inter-interpreter variability, the reference standard was based on consensus postoperative assessment by a panel of three dermatopathologists (S.E., K.E., S.K.) using the same frozen-section haematoxylin and eosin-stained slides used intraoperatively by the Mohs surgeons. Firstly, two dermatopathologists (S.E. and K.E.) assessed all stained sections independently (staggered by 1 month), while blinded to the AF–Raman instrument, Mohs surgeon and each other's assessments. In cases in which the two dermatopathologists did not agree, an external dermatopathologist (S.K.) provided an additional independent assessment, which was followed by a consensus panel meeting to decide on the final diagnosis. The study also compared the intraoperative assessment by the Mohs surgeon, as done in routine MMS to the reference standard, as a comparative technique to AF–Raman analysis.

Data analysis

The AF–Raman microspectroscopy results and the intraoperative assessment by MMS were compared with the reference standard after recruitment was completed (August 2023). The sensitivities, specificities, and positive (PPVs) and negative predictive values (NPVs) of AF–Raman microspectroscopy and MMS were calculated according to consensus postoperative histology, depending on whether the margins were clear or not. The 95% confidence intervals (CIs) were calculated using the Clopper–Pearson method. We also performed a detailed review of false-negative and false-positive cases, to better understand where the technology requires improvement.

Results

Study population

We obtained 130 first Mohs layers from 130 patients for evaluation by the AF–Raman instrument, of which 125 were successfully analysed. The five failed measurements were produced by incorrect loading of tissue cassettes in the instrument ($n=3$) or incorrect use of the instrument software ($n=2$).

The 125 specimens were excised from locations on the head and neck: nose ($n=72$), cheek ($n=20$), lip ($n=13$), eyelid ($n=9$), temple ($n=6$), forehead ($n=2$), eyebrow ($n=2$) and chin ($n=1$). The initial postoperative histology assessments by two of the three dermatopathologists were in agreement for 104 cases (83.2%). The remaining 21 cases were discussed at the consensus panel meeting (three dermatopathologists), which reached a final diagnosis for all 125 layers. Of the 125 layers, 36 had BCC-positive and 89 had BCC-negative margins. The 36 BCC-positive cases included nodular ($n=20$), superficial ($n=12$) and infiltrative ($n=4$) tumours.

Autofluorescence–Raman microspectroscopy and Mohs micrographic surgery

Both intraoperative histology during MMS and the AF–Raman instrument aimed to investigate 100% of the resection margin (deep and lateral). The results showed that the proportion of the specimen surface area investigated by the AF–Raman instrument depended on anatomical location: 87% (±8%) for the eyelids; 90% for the chin; 91% (±5%) for the nose; 92% (±5%) for the cheek; 93% (±6%) for the lip; 93% (±3%) for the temple; 93% (±1%) for the eyebrow; 94% (±1%) for the forehead. The main reason for not achieving full coverage was imperfect contact between the specimen surface and the cassette window, which was more pronounced for thicker specimens, such as those from the nose and chin. The second reason was the presence of superficial blood, which occluded the Raman signal. This was more pronounced in specimens from the eyelid, cheek and temple.

The performance in detecting residual BCC by the AF–Raman instrument and MMS (positive margins: 'yes' or 'no') were determined by calculating the sensitivity, specificity, PPV and NPV vs. consensus postoperative histology (Table 1). For the entire dataset, the AF–Raman instrument identified positive margins in 24 of 36 BCC-positive cases (67% sensitivity, 95% CI 49–82) and negative margins in 65 of 89 BCC-negative cases (73% specificity, 95% CI 63–82). The PPV was 50% (95% CI 35–65) and the NPV was 84% (95% CI 74–92).

For the same specimens, intraoperative assessment by the Mohs surgeons identified positive margins in 31 of 36 BCC-positive cases (86% sensitivity, 95% CI 70–95) and negative margins in 79 of 89 BCC-negative cases (89% specificity, 95% CI 81–95) (Table 1). The PPV was 76% (95% CI 60–88) and the NPV was 94% (95% CI 87–98).

Table 1 Performance of the autofluorescence–Raman microspectroscopy instrument and Mohs micrographic surgery (MMS) in detecting basal cell carcinoma

	TP (*n*)	FN (*n*)	TN (*n*)	FP (*n*)	Sensitivity (95% CI)	Specificity (95% CI)	PPV (95% CI)	NPV (95% CI)
Raman vs. reference	24	12	65	24	67% (49–82)	73% (63–82)	50% (39–61)	84% (74–92)
MMS vs. reference	31	5	79	10	86% (70–95)	89% (81–95)	76% (60–88)	94% (87–98)

CI, confidence interval; FN, false negative; FP, false positive, NPV, negative predictive value; PPV, positive predictive value; TN, true negative; TP, true positive.

The results reported for MMS were based on the intention to treat, with a layer being deemed BCC-positive if the surgeon excised an additional layer after the histopathological investigation of the first layer.

Typical examples of BCC-positive cases identified by AF–Raman microspectroscopy are presented in Figure 1. The results confirmed that all types of BCC can be detected by the AF–Raman instrument.

Discordant autofluorescence–Raman microspectroscopy cases

Of the 125 investigated layers, the results of 36 were discordant between AF–Raman analysis and the reference standard. Twelve cases were incorrectly classified as BCC-positive (false-positive) and 24 were incorrectly assessed as BCC-negative (false-negative). The AF–Raman maps showing discrepancies to the reference standard were inspected: the false-negative cases included superficial ($n=7$), nodular ($n=4$) and infiltrative BCC ($n=1$).

Of the 12 false-negative results, 8 were caused by inadequate contact between the tissue and the cassette window at the location of the tumour (leading to out-of-focus Raman measurements) and 3 were caused by occlusion of the residual tumour by superficial blood on the excision surface (Figure 2).

Only 1 of the 12 false-negative cases was due to incorrect classification by the Raman algorithm. The AF–Raman instrument did not detect a cluster of nodular BCCs within an approximately 100-μm area located in a region with numerous hair follicles and sebaceous units (Figure 3). This tumour was also missed by the Mohs surgeon at the time of surgery.

Of the 24 false-positive cases, 12 were caused by the presence of incipient hair follicles, 8 were caused by the presence of dense inflammation and 4 were single cases of seborrhoeic keratosis, benign naevi, viral warts and follicular hamartoma, respectively (Figure 4). Most false-positives were caused by incipient hair follicles. These were generally represented as single red regions <250 μm in the AF–Raman microspectroscopy map (Figure 4a). High-density accumulations of lymphocytes also resulted in false-positive assessments (Figure 4b), as did less common tissue structures that have not been encountered and measured in our previous studies: seborrhoeic keratosis, benign naevi, follicular hamartoma and viral warts (Figure 4c).

Discussion

When compared with the reference standard of consensus-derived postoperative histology, the AF–Raman instrument had a sensitivity of 67% and a specificity of 73% for the detection of residual BCC in our intention-to-treat analysis. These results are not good enough for clinical practice, using our current tissue-processing procedure. However, 11 of 12 false-negative diagnoses were caused either by the presence of blood (2 eyelid specimens and 1 from the upper cheek) or inadequate tissue–cassette window contact ($n=8$). Only one incomplete excision (false-negative) was caused by an incorrect classification by the Raman algorithm (Figure 3), a case that also resulted in a false-negative adjudication by the Mohs surgeon who assessed an intraoperative frozen section. Sensitivity of the AF–Raman microspectroscopy algorithm increased to 96% (95% CI 80–100%) if the specimens with poor tissue contact due to blood or lack of flattening were excluded. In a pilot study of 27 layers, we showed that splitting the specimens into two halves improved the tissue–cassette window contact ($>$ 95% of surface area investigated) and led to 1 false-negative result out of 9 true BCC-positive cases.[15] These results suggest a need to improve the tissue-processing methods (e.g. layer bisection to allow better surface contact, enhanced blood removal and standardized seating of specimens inside the AF–Raman cassettes), to improve the overall sensitivity of the AF–Raman assessment.

Twenty-four specimens produced false-positive AF–Raman microspectroscopy assessments, according to the reference standard. The main confounders were small incipient hair follicles (single red regions <250 μm) and high-density accumulations of lymphocytes. Seborrhoeic keratosis, benign naevi, follicular hamartoma and viral warts were not included in the original training database, resulting in incorrect classification by the Raman microspectroscopy model. Such misclassifications are likely to reduce over time as the Raman microspectroscopy model can be designed to be constantly updated by such 'learning' from false-positive cases.

Several other technologies have been investigated for the purpose of guiding skin cancer surgery, including confocal microscopy, optical coherence tomography (OCT) and two-photon fluorescence.[17–19] Unlike the AF–Raman instrument, these techniques produce images that require user interpretation, akin to histology. This has been shown to lead to variability in results, linked to user experience.[20]

Fluorescence confocal microscopy (FCM) has been used to detect BCC on excised skin specimens up to 2 cm in size, with 86–92% sensitivity and 60–90% specificity.[21–23] Two-photon fluorescence imaging (an extension of FCM) has been shown to produce real-time images of biopsies <6 mm, showing 93% concordance with paraffin histology.[24] However, FCM requires staining of the specimens with fluorophores, which may bleach and degrade the image quality, leading to further variability in diagnosis.[23] OCT was shown to have 67% sensitivity and 100% specificity in 18

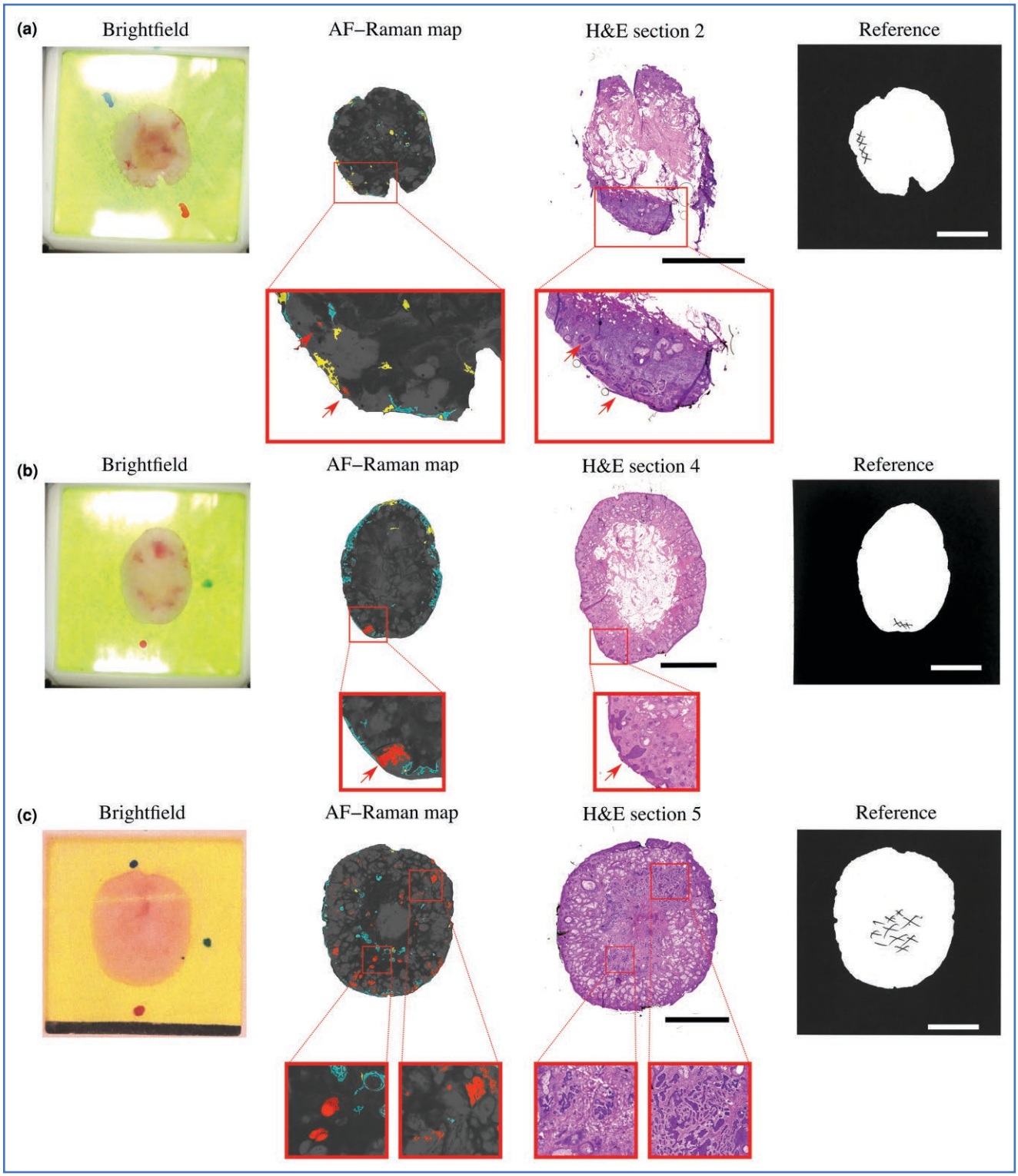

Figure 1 Typical examples of autofluorescence (AF)–Raman microspectroscopy results for basal cell carcinoma (BCC)-positive margins: (a) infiltrative, (b) superficial and (c) nodular. Brightfield images show the tissue layers placed in the AF–Raman cassette (coloured marks used to preserve orientation); AF–Raman maps show BCC as red regions and normal tissue as grey (yellow and blue regions indicate locations that were not adequately investigated owing to the presence of seeping blood or poor contact between tissue and the cassette window); frozen section haematoxylin and eosin (H&E)-stained histology images show the first occurrence of the tumour (BCC highlighted by red arrows in the insets), reference maps show the locations that were identified as BCC-positive by the reference standard as black crosses (consensus panel). Scale bars = 5 mm.

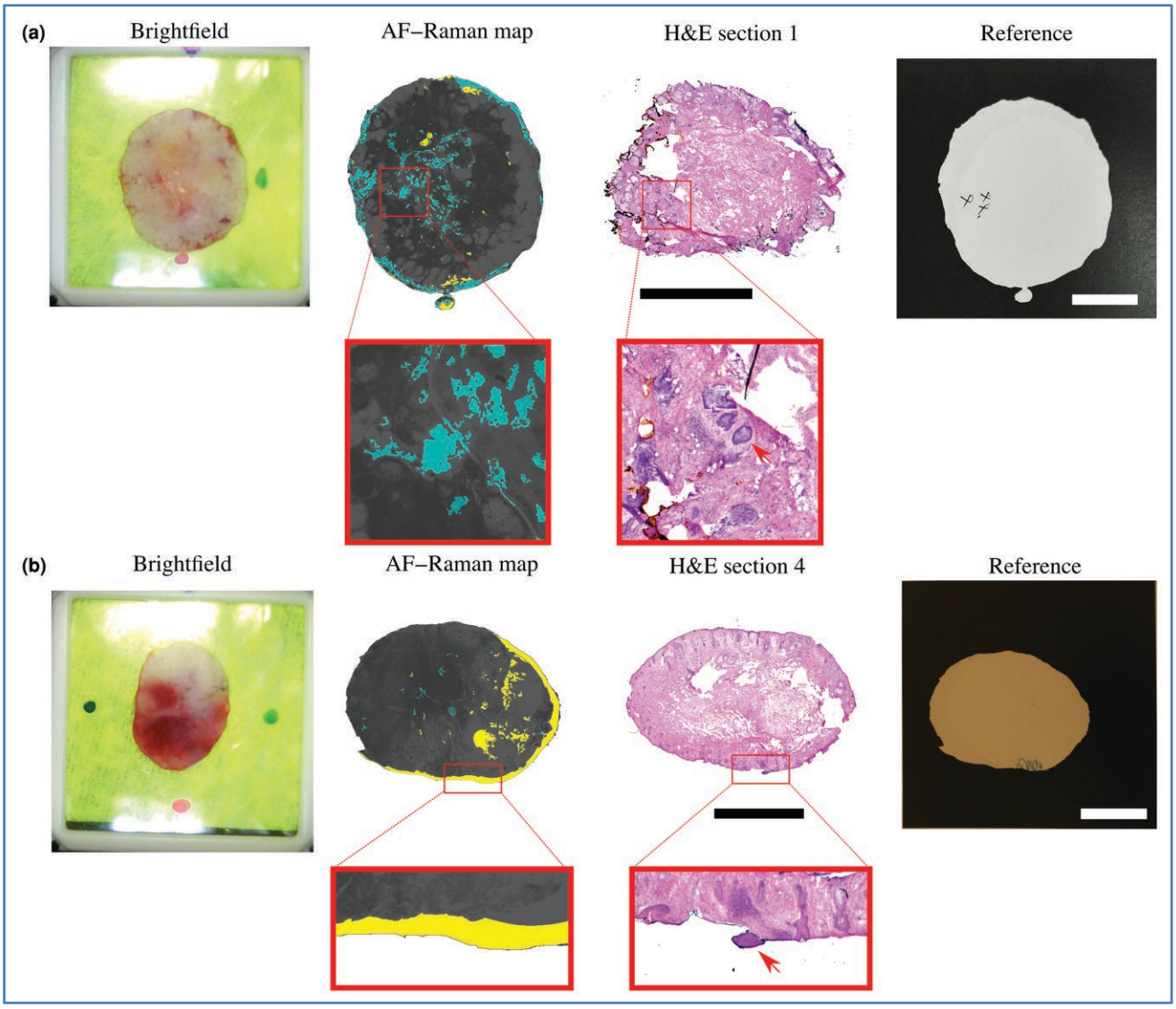

Figure 2 Assessment of surgical margins by autofluorescence (AF)–Raman microspectroscopy showing two examples of false-negative results. (a) False-negative result produced by improper contact between the specimen and the AF–Raman tissue cassette window, represented as a blue region in the AF–Raman map; (b) false-negative result produced by occlusion of residual tumour by superficial blood, represented as a yellow region in the AF–Raman map. Brightfield images show the tissue layers placed in the AF–Raman cassette with coloured markers used to preserve orientation and confirm the AF–Raman outcomes. No red regions can be observed in the AF–Raman maps, but basal cell carcinoma (BCC) can be identified in the frozen haematoxylin and eosin (H&E)-stained sections (highlighted by red arrows in the insets). Reference maps show the locations that were identified as BCC-positive by the reference standard. Scale bars = 5 mm.

fresh Mohs layers, although a larger sample size is required to substantiate these results.[17]

In this study, the AF–Raman instrument investigated approximately 91% of the excision surface for the layers. Irregular tissue surfaces have a negative impact on all other imaging technologies (including those mentioned above), leading to areas of the tissue surface being omitted.[21,25,26] Grizzetti and Kuonen reported that 11% of their set of FCM images contained < 90% of the tissue surface area.[26] Mu *et al.* excluded a third ($n = 54/187$) of the FCM images in their study, owing to poor image quality caused mostly by poor tissue–coverslip contact.[27]

van Lee *et al.* compared the accuracy of three Mohs surgeons and three dermatopathologists using a set of hand-picked frozen haematoxylin and eosin-stained sections.[28] On this set of specimens, the Mohs surgeons showed an average sensitivity of 92% and an average specificity of 68%. While variation is expected, owing to the differing datasets and interpretation methodologies between centres, the results reported here show that the AF–Raman instrument is comparable in performance to MMS, when ideal tissue processing is achieved.

User error resulted in five failed AF–Raman measurements. In practice, a user may reseat the cassette in the instrument or reload the analysis software and repeat the measurement. However, as this was not included in the current study protocol, repeat measurements were not carried out.

The AF–Raman instrument was able to investigate an average of 91% of the total excision surface for the layers in

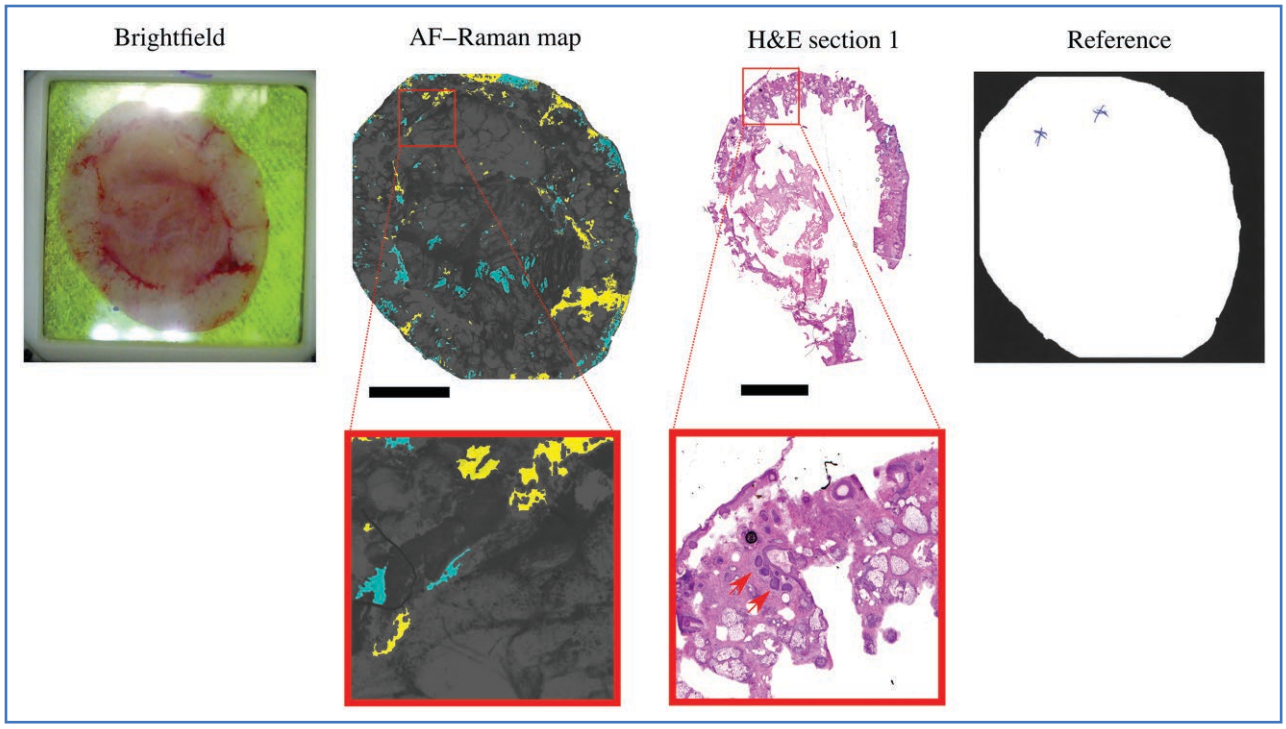

Figure 3 The only basal cell carcinoma (BCC)-positive margin not detected by the autofluorescence (AF)–Raman microspectroscopy instrument due to an incorrect classification by the Raman algorithm. Brightfield image shows the tissue layer placed in the AF–Raman cassette with a blue dot used to preserve orientation. There are no red segments denoting a BCC-positive detection in the AF–Raman map (yellow and blue regions indicate locations that were not adequately investigated due to the presence of blood or poor tissue-cassette window contact, respectively). A cluster of nodular BCCs located within an approximately 100-μm area in a region abundant in hair follicles and sebaceous units can be seen in the haematoxylin and eosin (H&E)-stained sections (red arrows) and is indicated in the reference map. Scale bars = 5 mm.

the study. The most commonly measured specimens were excised from the nose, cheek or lip ($n = 105/125$ layers). Specimens from these anatomical locations represent the largest proportion of cases treated at our centre. The only tissue type that was under-represented was the eyelid. One inclusion criterion for the study was for specimens to be blotted a minimum of 10 times, to remove superficial seeping blood.[16] Only 9 eyelid specimens could be blotted 10 times or more without a risk of tissue deterioration. A more effective blood-removal technique needs to be developed that does not deteriorate the tissue specimen and that can be performed within 5 min. With the current preprocessing procedure, the AF–Raman instrument is unsuitable for specimens resected from the periocular region, as all false-negative assessments produced because of occlusion by blood were resected from this region.

Our results indicated that the AF–Raman algorithm has the potential to produce a comparable sensitivity (96%, 95% CI 80–100) to MMS (86%, 95% CI 70–95%), when specimens for which BCC is occluded by superficial blood (periocular region) or are out of focus are excluded. A high sensitivity of tumour detection is required for all techniques that aim to guide surgery, as failure to ensure that the entirety of cancer is removed has been linked to higher recurrence rates.[28] However, the AF–Raman instrument produced a 16% lower specificity than MMS [73% (95% CI 63–82) vs. 89% (95% CI 81–95)]. In practice, use of the current AF–Raman instrument classification signal would therefore result in more healthy tissue being removed than MMS. The Raman classification model needs to be further trained with the inclusion of more representative Raman spectra from benign tissue structures (e.g. viral warts and follicular hamartoma), to further improve its specificity.

To ensure that the AF–Raman instrument operates at its maximum potential, several improvements in tissue processing are required (as is the case for any competing micrographic technology). The contact between tissue and cassette window has previously been shown to be improved by approximately 5% when specimens are measured as split-tissue samples rather than as full-face ones.[15] While the latter approach has the advantage of speeding up frozen section histology, there is no penalty in dividing the specimen into smaller fragments for AF–Raman analysis, as all fragments are analysed simultaneously. Thus, future use of AF–Raman instrument could be performed on bisected layers, which would allow for investigation of $>95\%$ of the resection surface.

Although the current instrument algorithm detects only BCC, during MMS, pathologists or surgeons examine lesions for the possibility of other malignancies, such as squamous cell carcinoma or melanoma that may coincidentally accompany the lesion. Thus, the training of the classification algorithms needs to be extended to include Raman spectra of such malignancies, to avoid the risk of overlooking them.

Because of the limitations related to tissue processing, the sensitivity of the AF–Raman device is not sufficiently high for intraoperative assessment during MMS. If better contact and blood removal can be achieved, then the AF–Raman instrument may become a viable alternative to frozen tissue processing for MMS and, potentially,

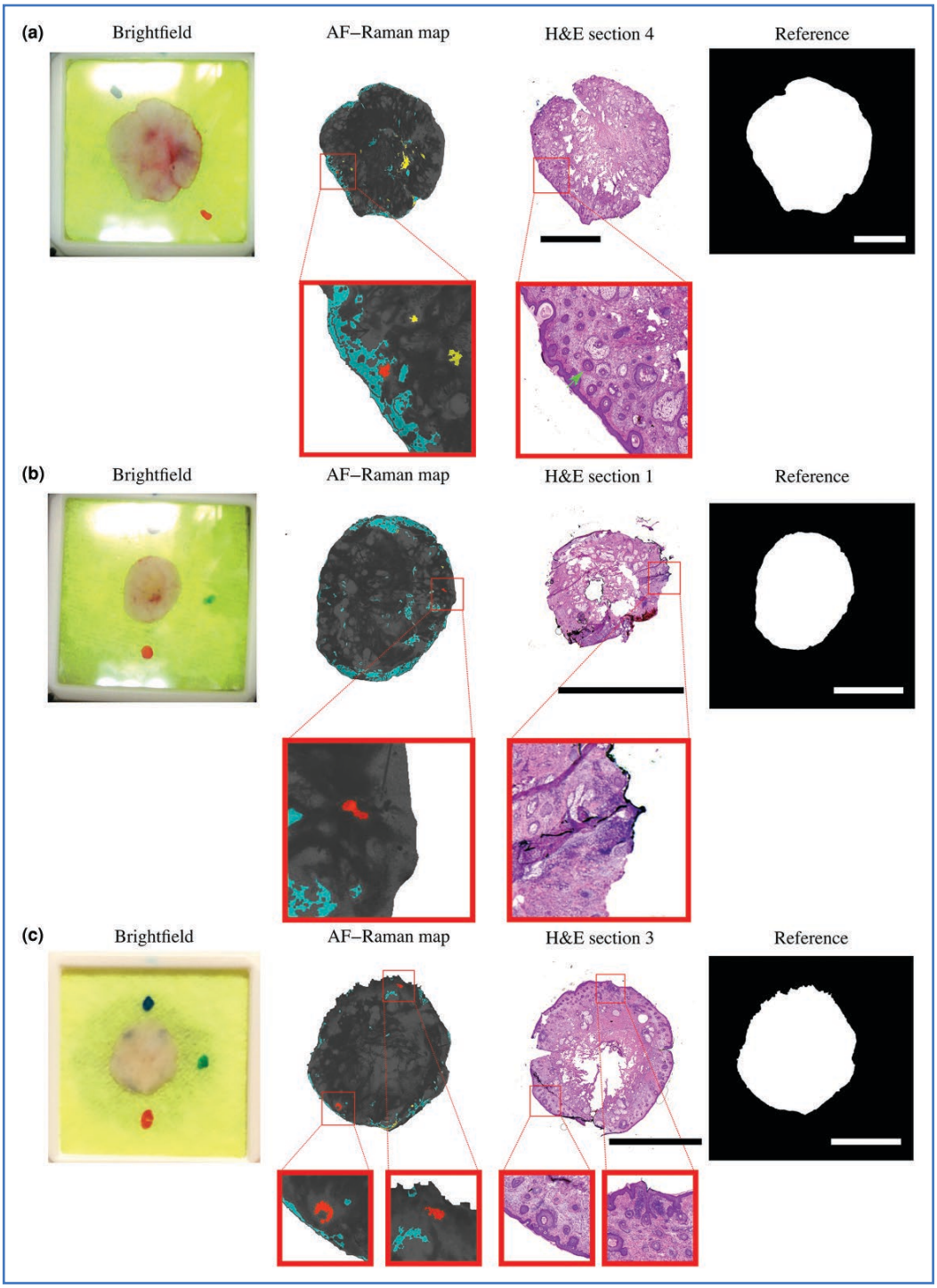

Figure 4 Examples of false-positive autofluorescence (AF)–Raman microspectroscopy assessments caused by (a) incipient hair follicles, (b) dense inflammation and (c) benign naevus and hair follicles. Brightfield images show the tissue layers placed in the AF–Raman cassette with coloured markers used to preserve orientation. Raman maps show red regions, even though there is no basal cell carcinoma present at the resection surface, as shown in the frozen haematoxylin and eosin (H&E)-stained sections and confirmed by the reference standard (no markings on the reference report). Scale bars = 5 mm.

for intraoperative margin control during WLE in centres with no access to MMS. Approximately 80% of people with BCC on the face and neck in the UK are treated by WLE and rely on paraffin-embedded histology to evaluate the surgical margins.[4] In such a setting, the AF–Raman instrument would allow for intraoperative micrographic assessment of the surgical margins, rather than having to wait 1–2 weeks for histology results. As the AF–Raman instrument provides an objective diagnosis based on the molecular characteristics of a tissue specimen, it can be used by any member of the surgery team after a short training period (days rather than months or years) directly on the fresh specimens, without the need of complex histology facilities.

Funding sources

This manuscript presents independent research commissioned by the National Institute for Health Research (NIHR) under its Research for Patients benefit programme (grant number PB-PG-0817-20019). The views expressed are those of the authors and not necessarily those of the NHS or the NIHR.

Conflicts of interest

S.V., A.K., H.C.W. and I.N. hold a patent related to Raman microspectroscopy technology. R.A.B., A.S., S.O., S.E., K.E., S.G., A.P., K.D.W. and S.K. declare no conflicts of interest.

Data availability

All data recorded are available upon request from the corresponding author.

Ethics statement

Ethical approval was granted by the Health Research Authority and Health and Care Research Wales (18/WM/0105). All patients provided written informed consent for participation in the study and the use of their de-identified, anonymized, aggregated data and their case details (including photographs) for publication.

Supporting Information

Additional Supporting Information may be found in the online version of this article at the publisher's website.

References

1 Sung H, Ferlay J, Siegel RL *et al.* Global cancer statistics 2020: GLOBOCAN estimates of incidence and mortality worldwide for 36 cancers in 185 countries. *CA Cancer J Clin* 2021; **71**: 209–49.
2 British Association of Dermatology. Basal cell carcinoma. 2023. Available at: https://www.bad.org.uk/pils/basal-cell-carcinoma (last accessed 11 July 2023).
3 Murray C, Sivajohanathan D, Hanna TP *et al.* Patient indications for Mohs micrographic surgery: a systematic review. *J Cutan Med Surg* 2019; **23**:75–90.
4 CancerData. Detailed Statistics from the 'Get Data Out' programme. Available at: https://www.cancerdata.nhs.uk/getdataout/skin (last accessed 14 May 2024).
5 Quazi SJ, Aslam N, Saleem H *et al.* Surgical margin of excision in basal cell carcinoma: a systematic review of literature. *Cureus* 2020; **12**:e9211.
6 Essers BA, Dirksen CD, Nieman FH *et al.* Cost-effectiveness of Mohs micrographic surgery vs surgical excision for basal cell carcinoma of the face. *Arch Dermatol* 2006; **142**:187.
7 Mosterd K, Krekels GA, Nieman FH *et al.* Surgical excision versus Mohs' micrographic surgery for primary and recurrent basal-cell carcinoma of the face: a prospective randomised controlled trial with 5-years' follow-up. *Lancet Oncol* 2008; **9**:1149–56.
8 Flohil SC, van Dorst AMJM, Nijsten T *et al.* Mohs micrographic surgery for basal cell carcinomas: appropriateness of "Rotterdam" criteria and predictive factors for three or more stages. *J Eur Acad Dermatol Venereol* 2012; **27**:907–11.
9 NHS Digital. Hospital Admitted Patient Care Activity, 2022–23. Available at: https://digital.nhs.uk/data-and-information/publications/statistical/hospital-admitted-patient-care-activity (last accessed 14 May 2024).
10 Bakker Schut TC, Caspers PJ, Puppels GJ *et al.* Discriminating basal cell carcinoma from its surrounding tissue by Raman spectroscopy. *J Invest Dermatol* 2002; **119**:64–9.
11 Larraona-Puy M, Ghita A, Zoladek A *et al.* Development of Raman microspectroscopy for automated detection and imaging of basal cell carcinoma. *J Biomed Opt* 2009; **14**:054031.
12 Kong K, Rowlands CC, Varma S *et al.* Diagnosis of tumors during tissue-conserving surgery with integrated autofluorescence and Raman scattering microscopy. *Proc Natl Acad Sci U S A* 2013; **110**:15189–94.
13 Boitor R, de Wolf C, Weesie F *et al.* Clinical integration of fast Raman spectroscopy for Mohs micrographic surgery of basal cell carcinoma. *Biomed Opt Express* 2021; **12**:2015–26.
14 Radu Boitor, Kong K, Shipp DW *et al.* Automated multimodal spectral histopathology for quantitative diagnosis of residual tumour during basal cell carcinoma surgery. *Biomed Opt Express* 2017; **8**:5749–66.
15 Boitor R, Varma S, Sharma A *et al.* Ex vivo assessment of basal cell carcinoma surgical margins in Mohs surgery by autofluorescence-Raman spectroscopy: a pilot study. *JEADV Clin Pract* 2023; https://doi.org/10.1002/jvc2.336 (Epub ahead of print).
16 RfPB project plan for testing reliability and diagnostic accuracy of Fast Raman device. Available at: https://www.nottingham.ac.uk/research/groups/cebd/documents/researchdocs/rfpb-project-plan-v6.1.pdf (last accessed 14 May 2024).
17 Durkin JR, Fine JL, Sam H *et al.* Imaging of Mohs micrographic surgery sections using full-field optical coherence tomography: a pilot study. *Dermatol Surg* 2014; **40**:266–74.
18 Bennàssar A, Vilata A, Puig S, Malvehy J. Ex vivo fluorescence confocal microscopy for fast evaluation of tumour margins during Mohs surgery. *Br J Dermatol* 2014; **170**:360–5.
19 Atak MF, Farabi B, Navarrete-Dechent C *et al.* Confocal microscopy for diagnosis and management of cutaneous malignancies. *Diagnostics (Basel)* 2023; **13**:854.
20 Kadouch DJ, Leeflang MM, Elshot YS *et al.* Diagnostic accuracy of confocal microscopy imaging vs. punch biopsy for diagnosing and subtyping basal cell carcinoma. *J Eur Acad Dermatol Venereol* 2017; **31**:1641–8.
21 Longo C, Pampena R, Bombonato C *et al.* Diagnostic accuracy of ex vivo fluorescence confocal microscopy in Mohs surgery of basal cell carcinomas: a prospective study on 753 margins. *Br J Dermatol* 2019; **180**:1473–80.
22 Peters N, Schubert M, Metzler G *et al.* Diagnostic accuracy of a new ex vivo confocal laser scanning microscope compared to H&E-stained paraffin slides for micrographic surgery of basal cell carcinoma. *J Eur Acad Dermatol Venereol* 2019; **33**:298–304.
23 Kose K, Alessi-Fox C, Rossi AM *et al.* An international 3-center training and reading study to assess basal cell carcinoma surgical margins with ex vivo fluorescence confocal microscopy. *J Cutan Pathol* 2021; **48**:1010–19.
24 Ching-Roa VD, Huang CZ, Ibrahim SF *et al.* Real-time analysis of skin biopsy specimens with 2-photon fluorescence microscopy. *J Am Acad Dermatol* 2022; **158**:1175–82.
25 Pérez-Anker J, Ribero S, Yélamos O *et al.* Basal cell carcinoma characterization using fusion ex vivo confocal microscopy: a promising change in conventional skin histopathology. *Br J Dermatol* 2020; **182**:468–76.
26 Grizzetti L, Kuonen F. Ex vivo confocal microscopy for surgical margin assessment: a histology-compared study on 109 specimens. *Ski Health Dis* 2022; **2**:e91.
27 Mu EW, Lewin JM, Stevenson ML *et al.* Use of digitally stained multimodal confocal mosaic images to screen for nonmelanoma skin cancer. *J Am Acad Dermatol* 2016; **152**:1335–41.
28 van Lee CB, Ip Vai Ching EEF, Nasserinejad K *et al.* Reliability of diagnosis from Mohs slides: interpersonal and intrapersonal agreement on basal cell carcinoma presence and histological subtype. *Br J Dermatol* 2016; **175**:549–54.